Research paper

Fabrication and Properties of Wood-Polylactic Acid Composite Filaments for Fused Deposition Modeling 3D Printing

Po-Heng Lin[1]   Chen-Lung Ho[2]   Cheng-Jung Lin[1]   San-Hsien Tu[1,3]

【 Summary 】

Three-dimensional (3D) printing is an emerging technology that is transforming manufacturing technology due to its unique advantages such as freeform fabrication, sustainability, and efficient manufacturing. In this study, we developed a wood flour (WF)/polylactic acid (PLA) composite filament for fused deposition modeling (FDM) 3D printing and analyzed its composite properties. Results showed that the tensile strength of the WF/PLA composite was considerably less than that of neat PLA. By adding 10 wt% of thermoplastic polyurethane (TPU) as a toughening agent, the elongation-at-break value of the WF/PLA composite was greater than that of neat PLA. This shows that the toughening agent could increase the ductility of the WF/PLA composite, leading to a better printing experience. We found a significant relationship among extrusion temperatures and dimensional stability of printed objects, whereas the surface roughness of specimens increased as the extrusion temperatures increased. A higher infill rate and greater extrusion layer height were both shown to give the printed object better dimensional stability.

Key words: wood-polylactic acid composite, fused deposition modeling, 3D printing, dimensional stability, surface roughness.

Lin PH, Ho CL, Lin CJ, Tu SH. 2022. Fabrication and properties of wood-polylactic acid composite filaments for fused deposition modeling 3D printing. Taiwan J For Sci 37(3):167-78.

[1] Division of Forest Utilization, Taiwan Forestry Research Institute, 53 Nanhai Rd., Taipei 10051, Taiwan. 林業試驗所森林利用組，100051臺北市南海路53號。

[2] Division of Wood Cellulose, Taiwan Forestry Research Institute, 53 Nanhai Rd., Taipei 10051, Taiwan. 林業試驗所木材纖維組，100051臺北市南海路53號。

[3] Corresponding author, e-mail:asan@tfri.gov.tw 通訊作者。

研究報告

木粉/聚乳酸複合3D列印線材的製造及性質分析

林柏亨[1)]　何振隆[2)]　林振榮[1)]　塗三賢[1,3)]

摘 要

　　三維(3D)列印是一項新興的技術，由於其獨特的優勢，例如形式自由、可持續性和效率性，正在改變傳統的製造技術。本研究開發了一種用於熔融沉積成型3D列印機的木粉/聚乳酸複合3D列印線材，並分析了它的性能。研究結果顯示，木粉/聚乳酸複合線材的拉伸強度遠低於純聚乳酸。在添加10%重量比的熱塑性聚胺酯(TPU)作為增韌劑後，木粉/聚乳酸複合線料的拉伸強度會顯著增加，它的斷裂伸長率也會大於純聚乳酸。這表示增韌劑可以增加木粉/聚乳酸複合線材的延展性，從而帶來更好的列印體驗。我們也發現列印時噴頭溫度與列印物件的尺寸穩定性間存在著顯著的相關，列印溫度愈高時，列印物件的尺寸穩定性愈好，但列印物件的表面粗糙度會隨著擠出溫度的升高而增加。較高的填充率和列印層高顯示會為列印物件提供更好的尺寸安定性。

關鍵詞：木粉/聚乳酸複合線材、熔融沉積成型、3D列印、尺寸安定性、表面粗糙度。

林柏亨、何振隆、林振榮、塗三賢。2022。木粉/聚乳酸複合3D列印線材的製造及性質分析。台灣林業科學37(3):167-78。

INTRODUCTION

Three-dimensional (3D) printing, also known as additive manufacturing (AM), is an emerging technology that is transforming manufacturing technology due to its unique advantages such as freeform fabrication, sustainability, and efficient manufacturing. Moreover, 3D printing shortens the time from design to production compared to subtractive or traditional manufacturing technology (Meteyer et al. 2014, Wimmer et al. 2015, Ou-Yang et al. 2018, Wasti and Adhikari 2020). Initially, 3D printing was developed as a means to prototype new products and shorten the product design cycle (Tisserat et al. 2015). Nowadays, 3D printing technology is being implemented in different sectors such as architecture and construction (Perkins and Skitmore 2015, Wu et al. 2016), the automotive and aerospace industries (Persons 2015), structural design (Melnikova et al. 2014),

healthcare and medical fields (Goyanes et al. 2016, Ozbolat et al. 2016), the fashion industry (Vanderploeg et al. 2017), and the food industry (Liu et al. 2017).

3D printing creates 3D objects in a layer-by-layer manner. The American Society for Testing and Materials (ASTM) methods categorize 3D printing into 7 major groups, including: binder jetting (BJ) or powder bed and inkjet head (PBIH), fused deposition modeling (FDM) or fused filament fabrication (FFF), stereolithography apparatus (SLA), electron beam melting (EBM), laminated object manufacturing (LOM), selective laser sintering (SLS), and digital light projection (DLP) (ASTM 2013).

Among the different types of additive manufacturing processes, FDM is a rapid, versatile, low-cost, commonly used 3D printing technique that can easily and promptly

fabricate complex-shaped parts (Tran et al. 2017). FDM is commonly used as a 3D printing methodology for its reliability, simplicity, affordability, minimal wastage, and material availability (Tao et al. 2017). In the FDM process, thermoplastic filaments, a conventionally used printable material, are fed to a liquefier head by pressure generated by a driver gear and a grooved bearing. The filament material is heated to its melting temperature region, extruded through the extrusion nozzle, and then deposited layer by layer onto the build platform. The deposited layers fuse together and solidify to form the required final object (Ngo et al. 2018, Xu et al. 2018).

The most commonly used thermoplastic materials are polylactic acid (PLA), acrylonitrile butadiene styrene (ABS), polycarbonate (PC), ethylene vinyl acetate (EVA), and polyamides (PAs) (Wasti and Adhikari 2020). The disadvantages of 3D structures built with FDM using neat PLA materials include the high cost, low strength, and easy distortion. These factors restrict the application of FDM in cost-effective, functional, and load-bearing applications as well as in large-scale production (Ning et al. 2015). Therefore, the development of new composite filaments for FDM is an important topic in the 3D printing industry (Tao et al. 2015).

PLA is the most widely used raw material in the FDM-based 3D printing process due to its biodegradability and environmentally friendly properties (Tümer and Erbil 2021). However, the production of PLA requires precise reaction conditions such as temperature and pressure, which accounts for higher energy consumption (Wasti and Adhikari 2020). Poor thermal and mechanical properties of PLA also limit its use for many engineering applications (Nguyen et al. 2018). Therefore, researchers have performed studies to develop new PLA composite filament materials for

FDM 3D printing.

Tao et al. (2017) developed a composite filament of PLA and 5 wt% of wood flour (WF) with a particle size of 14 μm for printing 3D objects by the FDM technique. Objects printed from composite filaments appeared more like wooden objects compared to those made from neat PLA filaments. However, due to the hydrophilic nature of WF and the hydrophobic nature of PLA, there were poor interfacial bonds, which resulted in clear gaps between the PLA and WF interfaces (Wasti and Adhikari 2020). Wimmer et al. (2015) found that the particle size of wood powder for blending with PLA should be ultrafine in order to prevent nozzle blocking during printing. Kariz et al. (2018) showed that increasing the wood concentration resulted in a decrement in the filament density. They found a slight increase in tensile strength with a 10% increase in the wood content, but further incremental increases in the wood content led to decreased tensile strength. Tisserat et al. (2015) found that wood-only composites were extremely brittle, so that the filaments often broke during printing, and more seriously, they typically clogged the extruder nozzle. Guo et al. (2018) explored different toughening agents for PLA/WF composite filaments, namely thermoplastic polyurethane (TPU), polycaprolactone (PCL), and poly(ethylene-co-octene) (POE), and found that among these, TPU showed the best compatibility with the WF/PLA composite. Ayrilmis (2018) examined the effects of the layer thickness on the surface roughness and wettability of 3D printed objects prepared from WF/PLA filaments and found direct impacts of the layer thickness on both properties. It was observed that with an increase in the layer thickness, both the surface roughness and wettability increased for 3D printed objects produced using WF/PLA filaments.

Wood fibers/flour are some of the most popular raw materials for manufacturing plant fiber/plastic composites. PLA, a compostable synthetic polymer produced using a monomer feedstock derived from corn starch, is an acceptable replacement for oil-derived plastics (Mukherjee and Kao 2011). Furthermore, wood wastes, such as sawdust, should be considered useful resources. In this study, we developed WF/PLA composite filaments for FDM 3D printing and analyzed their composite properties to extend the use of wood wastes. The purposes of this study were also to develop high value-added products to increase the use of wood wastes, achieve full use of wood materials, and meet the goals of a circular economy.

Today, there are thousands of models of 3D printers on the marker ranging in price from less than one hundred to several thousand dollars. This makes it possible for a wide audience of tinkerers and hobbyists to buy and use 3D printers at home (Landry 2021). Thousands of objects, including gadgets, hobby items, household implements, tools, and toys, have been designed and shared on the internet, and most of them are free to use for re-printing or modifying by anyone. Therefore, the dimensional stability of printed objects has become an important topic for 3D printer users. This study also discusses relationship among 3D printing parameters, such as extrusion temperatures, infill rates, and extrusion layer heights, with the dimensional stability of printed objects.

MATERIALS AND METHODS

Preparation of the WF/PLA composite filaments

The raw materials used in this study were China fir (*Cunninghamia lanceolata*) WF, Ingeo 4032D PLA thermoplastic pellets (NatureWorks, Minnetonka, MN, USA), and ISOTHANE 1085A TPU (Great Eastern Resins Industrial, Taichung, Taiwan). China fir WF was obtained from dried wood sawdust that was ground with a ball mill and sieve machine with a #200 sieve fraction (DLT-355, Dali, Chiayi, Taiwan). The mean particle size of the WF was 71 μm.

Raw materials were initially dehydrated (at 103℃) for 6 h to eliminate moisture, then blended with 15 wt% WF, 75 wt% PLA, and 10 wt% TPU in a twin-screw extruder (Kobelco, PIDC, Taichung, Taiwan). This created strands that were pelletized for subsequent processing with a single-screw extruder to create the final composite filament strands for the 3D printer. The WF/PLA composite filaments were 1.75 mm in diameter.

Examination of the properties of WF/PLA composite filaments

The neat PLA filaments and WF/PLA composite filaments were printed as test specimens according to the ASTM D638 Type IV bar standard for the tensile strength test. 3D printing was conducted with a dual-extruder printer (Raise3D Pro2Plus, Irvine, CA, USA) fitted with nozzles with 0.4-mm-diameter openings that employed the following characteristics: an extrusion layer height of 0.2 mm, infill rates of 100%, an extrusion temperature of 220℃, a build plate temperature of 60℃, an extrusion speed of 50 mm s^{-1}, and a build direction of a unidirectional pattern running parallel to the longitudinal direction.

The WF/PLA composite filaments were also printed as 30 × 30 × 5-mm cuboid specimens for the printing parameter test. The characteristics employed were as follows: infill rates of 20, 50, and 100%; extrusion temperatures of 180, 190, 200, 210, and 220℃; and extrusion layer heights of 0.15, 0.2, and 0.25 mm. In total, there were 45 cuboid

specimens with different printing parameters, and 3 replicates were printed for each cuboid specimen. Specimens were printed with a bi-directional pattern cross-hatched at opposing diagonal angles to the longitudinal direction, and a schematic representation of a printed cuboid specimen is shown as Figure 1. All cuboid specimens were immersed in water for 24 h. Then we calculated the water-absorption rates (WARs) and length-swelling rates (LSRs) to compare their dimensional stability.

Tensile properties of the specimens were measured with a universal testing machine (Shimadzu AGS-X 50, Kyoto, Japan). Three replicates were prepared for mean value calculations. Stress-strain curves and elasticity moduli were obtained.

The melt flow index (MFI) was measured in an MFI tester (DH-MI-VP, Dahometer, Guangdong, China) to ascertain the MFI of the filaments following the ASTM D1238 standard. A standard load of 2.16 kg was applied to the filaments with a 2.1-mm-diameter die at a temperature of $190°C$. The flow of material was observed for 10 min. The material weight that flowed through the die cavity for 10 min gave the MFI in g $(10 \text{ min})^{-1}$.

Thermogravimetric analyses (TGAs) of specimens were performed in a thermogravi-metric analyzer (Shimadzu DTG-60). Samples of about 4 mg, which were placed in a 40-μL aluminum pan, were heated from 30 to $600°C$ for the TGA, at a rate of $10°C \text{ min}^{-1}$, to observe their thermal degradation behaviors. Throughout the entire procedure, the N_2 flow rate was 40 mL min^{-1}.

A scanning electron microscope (SEM) (TM3000, Hitachi, Tokyo, Japan) was used to examine the microstructure of gold-coated filament specimens. The accelerating voltage was 15 kV. SEM images were obtained at different zones of each sample.

The surface roughness of specimens was measured with a contact-type surface texture measuring instrument (SURFCOM TOUCH 50, Tokyo Seimitsu, Tokyo, Japan). The arithmetical mean roughness (Ra), maximum height (Ry), and 10-point mean roughness (Rz) of printed specimens with different extrusion temperatures, fill rates, and layer heights were measured perpendicular to the longitudinal direction of the sample.

RESULTS AND DISCUSSION

Properties of the WF/PLA composite filaments
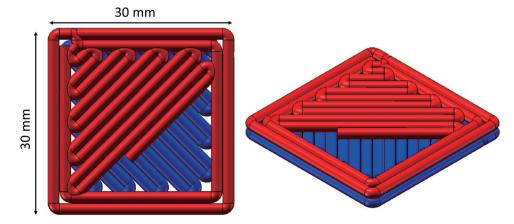
The specific gravity of the WF/PLA

Fig. 1. Schematic representation of a printed cuboid specimen.

filaments was 1.20, which was slightly lower than that of neat PLA filaments. The MFI of WF/PLA filaments was 7.23 g (10 min)$^{-1}$, as shown in Table 1, and compared to 8.90 g (10 min)$^{-1}$ for neat PLA, the MFI value had decreased by about 18.7%. The MFI is a simple measurement of the quantity of polymer pushed through a die of specified dimensions at a set temperature within 10 min. It is frequently used to compare grades of the same polymer, as it gives an indication of the molecular weight present in a certain batch or grade (Spear et al. 2015). Wang et al. (2017) investigated the MFI of 7 commercial PLA filaments. The MFIs of those PLA filaments ranged 4.3~16.4 g (10 min)$^{-1}$. They suggested putting forward a threshold value of 10 g (10 min)$^{-1}$ for successful printing (190~220℃), enabling rapid and practical screening of PLA materials. Materials with a sufficiently high MFI (> 10 g (10min)$^{-1}$) showed good flow properties with no clogging at the nozzle. However, high-MFI filaments easily curled upwards after extrusion against the print head, twisting, rather than sticking to the platform. The WF/PLA filament of this study was suitable for common FDM 3D printing, but a higher extrusion temperature was needed to prevent clogging at the nozzle.

The TGA-DTG curves in Figure 2 show that the starting thermal degradation temperature of WF was about 230℃, and the maximum decomposition rate shown in the DTG curve peaked around 360℃, while the starting thermal degradation temperature of PLA was about 310℃, which was higher than that of WF. The WF/PLA composite also decomposed at about 310℃, which showed that the WF had little effect on the thermal stability of the composites. With the addition of WF, the final thermal decomposition residual ratio of the WF/PLA composites increased more than that of PLA, due to the higher thermal decomposition residual ratio of WF. Tao et al. (2017) obtained similar results for the thermal stability of WF/PLA composites. The working temperature of a 3D printer with PLA filaments is around 180~230℃. As a result, the TGA showed that the WF/PLA composite filaments of this study could meet the temperature requirement of a 3D printer without unnecessary thermal decomposition.

The mechanical properties of the tensile test results are also summarized in Table 1. As shown in Table 1, the tensile strength (TS) value of the WF/PLA composite was considerably less than that of neat PLA. The TS value of the WF/PLA composite was only 46.56% that of neat PLA. The addition of TPU should have caused a decrease in strength; however, the reduction in TS values in the WF/PLA composite was typically due to poor interfacial bonding between the hydrophobic PLA and hydrophilic WF (Wasti and Adhikari 2020). The poor interfacial bonding between the PLA and WF is shown in Figure 3. The fracture surface of the WF/PLA composite was rough. WF could be encapsulated by the PLA matrix, while clear gaps could be observed in certain areas between the WF and PLA interfaces.

Guo et al. (2018) obtained similar poor

Table 1. Melt flow index (MFI) and mechanical properties of filaments

Sample	Specific gravity	MFI (g (10 min^{-1}))	TS (MPa)	YM (MPa)	ELO (%)
Pure PLA	1.24	8.90 (0.01)[1]	38.78 (13.27)	873.77 (21.63)	5.82 (0.17)
WF/PLA	1.20	7.23 (0.08)	18.06 (0.15)	628.20 (8.11)	10.53 (0.93)

Numbers in parentheses are standard deviations. TS, tensile strength; YM, Young's modulus; ELO, elongation at break.

mechanical property results with an increase in the poplar WF content in PLA. The elongation-at-break (ELO) value of the WF/PLA composite was significantly larger than that of neat PLA, likely due to the contribution of 10 wt% of TPU as the toughening agent. A toughening agent usually increases the overall ductility of a polymer over a wide temperature range but also improves resistance to notch sensitivity and toughness of thick sections (Keskkula and Paul 2018).

Dimensional stability

In this study, 5 extrusion temperatures of 180, 190, 200, 210, and 220℃ were investigated. Results are shown in Table 2.

LSR values in the length (LSR-L) direction of these specimens ranged 0.11%~0.23%, LSR values in the thickness (LSR-T) direction ranged 0.11%~0.36%, and WAR values ranged 2.37%~3.67%. LSR-T values tended to be larger than those in the length direction; this shows that the interfacial bonding between layers was poorer than that within layers. A higher extrusion temperature led to a higher LSR-T value. However, there was no significant relationship between extrusion temperatures and WAR values.

Table 3 shows LSR and WAR values of the WF/PLA composite filaments at different infill rates. LSR-L values ranged 0.10%~0.21%, LSR-T values ranged
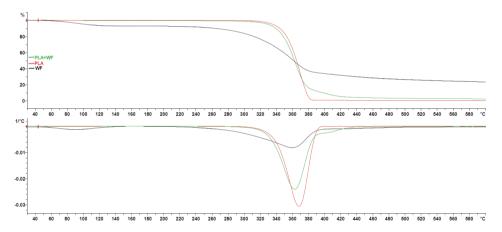

Fig. 2. Thermogravimetric analysis (TGA)-DTG curves of wood flour (WF), polylactic acid (PLA), and the WF/PLA composite (PLA+WF).

Table 2. Length-swelling rates (LSRs) and water-absorption rates (WARs) of wood flour (WF)/polylactic acid (PLA) composite specimens at different extrusion temperatures

Temp. (℃)	LSR-L (%)	LSR-T (%)	WAR (%)
180	0.23^A (0.05)	0.11^A (0.20)	2.53^A (1.11)
190	0.18^A (0.10)	0.28^A (0.20)	3.21^A (1.20)
200	0.14^B (0.06)	0.30^B (0.23)	3.34^A (1.42)
210	0.20^A (0.10)	0.35^B (0.23)	3.67^A (2.46)
220	0.11^B (0.09)	0.36^B (0.20)	2.37^A (1.02)

LSR-L, LSR in the length direction; LSR-T, LSR in the thickness direction. Numbers in the parentheses are standard deviations. Different letters (A and B) in a column indicate a significant difference at the 0.05 level by an ANOVA and Tukey's test.

0.21%~0.35%, and WAR values of these specimens ranged 1.69%~4.24%. The LSR-L value was 0.21% at an infill rate of 20%, and decreased to 0.10% at an infill rate of 100%. LSR-T and WAR values also decreased as the infill rate increased. Results showed that increasing the infill rate of a printed specimen decreased both LSR and WAR values, which meant that specimens with higher infill rates had better dimensional stability.

LSR and WAR values of the WF/PLA composite filaments at different extrusion layer heights are shown in Table 4. LSR-L values ranged 0.15%~0.21%, LSR-T values ranged 0.24%~0.30%, and WAR values of these specimens ranged 2.74%~3.78%. Results showed that increasing the extrusion layer height of the printed specimens decreased LSR-L values, while no similar trend was found in the thickness direction. Increasing the extrusion layer height led to a decrease in WAR values, too. Results indicated that specimens with higher extrusion layer heights had better dimensional stability.

Surface roughness

Differences in surface roughness were analyzed using an analysis of variance (ANOVA). Comparisons of the arithmetical mean roughness (Ra), maximum height (Ry), and 10-point mean roughness (Rz) at different extrusion temperatures are shown in Table 5. It shows that the surface roughness of specimens increased as the extrusion temperature increased. According to Tukey's test results, Ra, Ry, and Rz values at 210~220℃ extrusion temperatures were significantly larger than those at 180~200℃. The majority of changes in the surface roughness occurred at 210℃. However, no statistically significant differences of extrusion temperatures at 180~200℃ were found.

The fill rate of 3D printing is the most important criterion that determines the strength of the model (Kaptan and Kartal 2020), but fill rates do not significantly affect the surface roughness of specimens (Table 6). Differences in the surface roughness at different printing layer heights are shown in Table 7. The Ra value with a layer height of 0.15 mm was

Table 3. Length-swelling rates (LSRs) and water-absorption rates (WARs) of wood flour (WF)/polylactic acid (PLA) composite specimens at different infill rates

Infill rate (%)	LSR-L (%)	LSR-T (%)	WAR (%)
20	0.21[A] (0.07)	0.35[A] (0.22)	4.24[A] (1.63)
50	0.20[A] (0.09)	0.29[A] (0.22)	3.14[B] (1.10)
100	0.10[B] (0.05)	0.21[B] (0.13)	1.69[C] (0.35)

LSR-L, LSR in the length direction; LSR-T, LSR in the thickness direction. Numbers in parentheses are standard deviations. Different letters (A, B, and C) in a column indicate a significant difference at the 0.05 level by an ANOVA and Tukey's test.

Table 4. Length-swelling rates (LSRs) and water-absorption rates WARs) of wood flour (WF)/polylactic acid (PLA) composite specimens at different extrusion layer heights

Layer height (mm)	LSR-L (%)	LSR-T (%)	WAR (%)
0.15	0.21[A] (0.09)	0.29[A] (0.20)	3.78[A] (2.13)
0.20	0.15[A] (0.07)	0.24[A] (0.16)	2.78[A] (1.15)
0.25	0.15[A] (0.10)	0.30[A] (0.19)	2.74[A] (1.03)

LSR-L, LSR in the length direction; LSR-T, LSR in the thickness direction. Numbers in parentheses are standard deviations. Different letters (A and B) in a column indicate a significant difference at the 0.05 level by an ANOVA and Tukey's test.
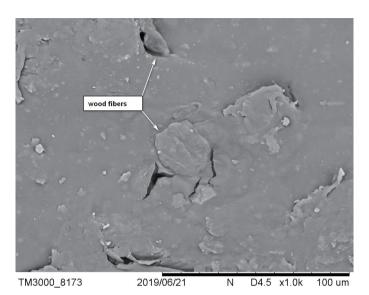
TM3000_8173   2019/06/21   N   D4.5   x1.0k   100 um

Fig. 3. SEM image of a specimen showing clear gaps between the wood flour (WF) and polylactic acid (PLA) interfaces.

Table 5. Surface roughness of wood flour (WF)/polylactic acid (PLA) composite specimens at different extrusion temperatures

Temp. (℃)	Ra (μm)	Ry (μm)	Rz (μm)
180	3.63[A] (1.03)	21.48[A] (6.59)	15.50[A] (4.25)
190	3.73[A] (1.12)	23.68[A] (7.49)	16.50[A] (5.51)
200	4.70[A] (1.67)	27.51[A] (7.25)	19.50[A] (6.06)
210	5.77[C] (2.66)	33.81[B] (12.16)	24.09[B] (10.17)
220	5.66[B] (1.99)	41.17[B] (18.65)	27.46[B] (14.24)

Ra, arithmetical mean roughness; Ry, maximum height; Rz, 10-point mean roughness. Numbers in parentheses are standard deviations. Different letters (A and B) in a column indicate a significant difference at the 0.05 level by an ANOVA and Tukey's test.

Table 6. Surface roughness of wood flour (WF)/polylactic acid (PLA) composite specimens at different fill rates

Infill rate (%)	Ra (μm)	Ry (μm)	Rz (μm)
20	5.43[A] (2.73)	32.90[A] (14.77)	23.92[A] (12.19)
50	4.76[A] (1.53)	31.19[A] (13.67)	20.88[A] (9.39)
100	4.71[A] (1.78)	30.54[A] (13.29)	20.85[A] (9.40)

Ra, arithmetical mean roughness; Ry, maximum height; Rz, 10-point mean roughness. Numbers in parentheses are standard deviations. Different letters (A and B) in a column indicate a significant difference at the 0.05 level by an ANOVA and Tukey's test.

significantly larger than those at other heights. However, we found no significant differences in Ry or Rz values for different layer heights.

These results were similar to those reported by Elkaseer et al. (2020), who found that the printing temperature slightly increased the

Table 7. Surface roughness of wood flour (WF)/polylactic acid (PLA) composite specimens at different layer heights

Layer height (mm)	Ra (μm)	Ry (μm)	Rz (μm)
0.15	5.92[A] (2.79)	35.51[A] (16.31)	24.89[A] (12.35)
0.2	4.04[B] (1.86)	28.44[A] (16.61)	19.41[A] (12.44)
0.25	4.93[B] (0.52)	30.68[A] (4.02)	21.36[A] (2.89)

Ra, arithmetical mean roughness; Ry, maximum height; Rz, 10-point mean roughness. Numbers in parentheses are standard deviations. Different letters (A and B) in a column indicate a significant difference at the 0.05 level by an ANOVA and Tukey's test.

roughness, although the infill percentage had no influence on the surface roughness.

CONCLUSIONS

In this study, we developed WF/PLA composite filaments for FDM 3D printing and analyzed the composite properties. Results show that the specific gravity of the WF/PLA filaments was slightly lower than that of neat PLA filaments. The MFI of WF/PLA filaments was also lower than that of neat PLA. The tensile strength (TS) value of the WF/PLA composite was considerably less than that of neat PLA. By adding 10 wt% of TPU as the toughening agent, the elongation-at-break value of the WF/PLA composite was larger than that of neat PLA. There was no significant relationship among extrusion temperatures and dimensional stability, whereas the surface roughness of specimens increased as the extrusion temperature increased. Both a higher infill rate and greater extrusion layer height yielded printed objects with better dimensional stability. In consideration of processing time and energy consumption, the suitable printing parameter settings for this WF/PLA filament include an extrusion temperature of 200℃, an infill rate of 50%, and a layer height of 0.2 mm.

ACKNOWLEDGEMENTS

REFERENCES

Ayrilmis N. 2018. Effect of layer thickness on surface properties of 3D printed materials produced from wood flour/PLA filament. Polym Test 71:163-6.

Elkaseer A, Schneider S, Scholz SG. 2020. Experiment-based process modeling and optimization for high-quality and resource-efficient FFF 3D printing. Appl Sci 10:2899.

Goyanes A, Det-Amornrat U, Wang J, Basit AW, Gaisford S. 2016. 3D scanning and 3D printing as innovative technologies for fabricating personalized topical drug delivery systems. J Ctrl Rel 234:41-8.

Guo R, Ren Z, Bi H, Song Y, Xu M. 2018. Effect of toughening agents on the properties of poplar wood flour/poly (lactic acid) composites fabricated with fused deposition modeling. Eur Polym J 107:34-45.

Kaptan A, Kartal F. 2020. The effect of fill rate on mechanical properties of PLA printed samples. J Inst Sci Tech 10(3):1919-27.

Kariz M, Sernek M, Obu´cina M, Kuzman MK. 2018. Effect of wood content in FDM filament on properties of 3D printed parts. Mater Today Comm 14:135-40.

Keskkula H, Paul DR. 1994. Toughening agents for engineering polymers. In: Collyer AA, editor. Rubber toughened engineer plastics. Dordrecht, the Netherlands. Springer. p 136-64.

Liu Z, Wang Y, Wu B, Cui C, Guo Y, Yan C. 2019. A critical review of fused deposition modeling 3D printing technology in manufacturing polylactic acid parts. Int J Adv Manuf Technol 102:2877-89.

Liu Z, Zhang M, Bhandari B, Wang Y. 2017. 3D printing: printing precision and application in food sector. Trends Food Sci Technol 69:83-94.

Landry M. 2021. Practical uses for a 3D printer at home. Available at https://bootcamp. uxdesign.cc/3-practical-uses-for-a-3d-printer-at-home-8bc2e61e9e2d. Accessed 2021 July 21.

Melnikova R, Ehrmann A, Finsterbusch K. 2014. 3D printing of textile-based structures by fused deposition modelling (FDM) with different polymer materials. IOP Conf Ser Mater Sci Engin 62:012018.

Meteyer S, Xu X, Perry N, Zhao YF. 2014. Energy and material flow analysis of binder-jetting additive manufacturing processes. Proc CIRP 15:19-25.

Mukherjee T, Kao N. 2011. PLA based biopolymer reinforced with natural fibre: a review. J Polym Environ 19:714-25.

Ning F, Cong W, Qiu J, Wei J, Wang S. 2015. Additive manufacturing of carbon fiber reinforced thermoplastic composites using fused deposition modeling. Compos Part B Engin 80:369-78.

Ngo TD, Kashani A, Imbalzano G, Nguyen KTQ, Hui D. 2018. Additive manufacturing (3D printing): a review of materials, methods, applications and challenges. Compos Part B Engin 143:172-96.

Nguyen NA, Barnes SH, Bowland CC, Meek KM, Littrell KC, Keum JK, et al. 2018. A path for lignin valorization via additive manufacturing of high-performance sustainable composites with enhanced 3D printability. Sci Adv 4:4967.

Ou-Yang Q, Guo B, Xu J. 2018. Preparation and characterization of poly (butylene succinate)/polylactide blends for fused deposition modeling 3D printing. ACS Omega 3:14309-17.

Ozbolat IT, Peng W, Ozbolat V. 2016. Application areas of 3D bioprinting. Drug Discov Today 21:1257-71.

Perkins I, Skitmore M. 2015. Three-dimensional printing in the construction industry: a review. Int J Constr Manage 15:1-9.

Persons T. 2015. 3D printing: opportunities, challenges, and policy implications of additive manufacturing. Available at https://www.gao. gov/assets/680/670960.pdf. Accessed 2021 July 25.

Spear MJ, Eder A, Carus M. 2015. Wood polymer composites. In: Martin A, editor. Wood composites. Amsterdam, the Netherlands. Woodhead Publishing. p 195-249.

Tao Y, Wang H, Li Z, Li P, Shi SQ. 2017. Development and application of wood flour-filled polylactic acid composite filament for 3d printing. Materials 10(4):339.

Tisserat B, Liu Z, Finkenstadt V, Lewandowski B, Ott S, Reifschneider L. 2015. 3D printing biocomposites. J Plastics Res Online 2015:1-3.

Tran TN, Bayer IS, Heredia-Guerrero JA, Frugone M, Lagomarsino M, Maggio F. 2017. Cocoa shell waste biofilaments for 3D printing applications. Macromol Mater Engin 302:1-10.

Tümer EH, Erbil HY. 2021. Extrusion-based 3D printing applications of PLA composites: a review. Coatings 11:390-3.

Wang S, Capoen L, D'hooge D, Cardon L. 2017. Can the melt flow index be used to predict the success of fused deposition modelling of commercial poly(lactic acid) filaments into 3D printed materials? Plastics Rubber Composites 47:1-8.

Wasti S, Adhikari S. 2020. Use of biomaterials for 3D printing by fused deposition modeling technique: a review. Front Chem 8:315-8.

Welzel T, Ertane EG, Dorner-Reisel A, Matner V, Baran O, Svoboda S. 2018. Process-

ing and wear behaviour of 3D printed PLA reinforced with biogenic carbon. Adv Tribol 2018:1-11.

Wimmer R, Steyrer B, Woess J, Koddenberg T, Mundigler N. 2015. 3D printing and wood. Pro Ligno 11(4):145-50.

Wu P, Wang J, Wang X. 2016. A critical review of the use of 3-D printing in the construction industry. Autom Constr 68:21-31.

Xu W, Pranovich A, Uppstu P, Wang X, Kronlund D, Hemming J. 2018. Novel biorenewable composite of wood polysaccharide and polylactic acid for three dimensional printing. Carbohydr Polym 187:51-8.